Research article Rapports De Pharmacie Vol.1 (3), 2015, 150-162
ISSN: 2455-0507

DEVELOPMENT AND OPTIMIZATION OF TWEEN 20/ SPAN 20 NIOSOMES OF MORIN HYDRATE

Chen Yan Cong[1], Jaya Raja Kumar[2]
[1]Research student of Pharmacy, AIMST University, Semeling, Bedong, Malaysia
[2]Faculty of Pharmacy, AIMST University, Semeling, Bedong, Malaysia

ABSTRACT
Morin hydrate (MH), one of the bioflavonoid has been identified in a number of fruits, vegetables, and herbs of the moraceae family. Several studies showed that morin has neuroprotective action in Parkinson's disease. Niosomes capable on entrapping and retaining morin hydrate were prepared by ether injection method. The objectiveof this study is preparation and optimization of morin hydrate loaded nanocarrier system. A 3-factor, 2-level Box-Behnken design was used to optimize the process parameters including Drug (A), Tween 20 (B) and Span 20 (C). Four dependent variables viscosity, size, cumulative drug release and drug loading efficacy were measured as responses. The accurate model produced for % CDR(R3) was found to be significant with F-value of 212.81 ($p < 0.0001$) and R^2 value of 0.9964. The independent variables A, B, C has significant effects on the % CDR, since the P-values less than 0.0500 represent the significant model. The studentized residuals are located by dividing the residuals by their standard deviations. According to evident from this figure R1, R2, R3 and R4, the points are scattered randomly between the outlier detection limits - 4.5 to + 4.5.
Keywords: Morin hydrate, Niosomes, HPLC, Box-Cox Plot, Tween 20, Polynomial equations

INTRODUCTION
Morin hydrate (3,5,7,2',4'-pentahydroxyflavone), one ofthe bioflavonoid has been recognized in a number of fruits, vegetables, and herbs of the moraceae family [1,2]. Numerous studies showed that morin has neuroprotective action in Parkinson's disease [1]. It induces apoptosis in hepatocellular carcinogenesis model [3], inhibits the growth of HL-60 cells and breastcancer resistance protein (ABCG2)-mediated transport [4, 5] in addition to its dual action as a hypouricemic agent and xanthine oxidase inhibitor [6]. On concurrent practice Morin also has been proved to alter the pharmacokinetics of some drugs by improving their oralbioavailability in rats [7, 8].

Non-ionic surfactant-based vesicles (niosomes) are made from the self-assembly of non-ionic amphiphiles in aqueous media resultant in closed bilayer structures. Bilayer structures are analogous to phospholipid vesicles (liposomes) and are capable to encapsulate aqueous solutes and assist as drug carriers. The low cost, better stability and resultant comfort of storage of non-ionic surfactants [9] has lead to the mistreatment of these compounds as substitutes to phospholipids. Surfactant forming niosomes are biodegradable, non-immunogenic and biocompatible. Adjustable functions have been reported for vesicular systems such as skin drugdelivery systems. They can afford a localized depot in the skin and reduce the amounts of drug permeating into the systemic circulation, thus reducing the unwantedeffects [10]. They may also deliver targeted delivery through the appendageal pathway (hair follicles and sweat ducts)[11]. Numerous mechanisms have been used to explain the capability of niosomes to modulate drug transfer through the skin, e.g. adsorption and fusion of niosomes on the surface of the skin, leading to a high thermodynamic activity gradient of the drug at the interface, which is the driving force for the permeation of a lipophilic drug, and the reduction of the barrier properties of stratum corneum resulting from the property of vesicles as a penetration enhancer[12]. Several drugs such as estradiol [13], tretinoin [14] and dithranol [15] have been effectively encapsulated in niosomes for topical application and these systems have been reported to

Address for correspondence:
Chen Yan Cong,
Research student of Pharmacy,
AIMST University, Semeling, Bedong,
Malaysia.
Email: jayaraj2775@gmail.com

give a substantial drug release [16]. Additionally, in several studies it has been told that compared to conventional dosage forms, vesicular formulations exhibited an enhanced cutaneous drug bioavailability[17].

Cholesterol influences the physical properties and structure of niosomes may be due to its interaction with the nonionic surfactants [18]. The interaction is of biological interest, cholesterol is constantly present in biological membranes here it influences membrane properties such as aggregation, ion permeability, fusion processes,elasticity, enzymatic activity, size and shape. The effect of cholesterol in lipid bilayers is mainly to modulate their cohesion and mechanical strength and their permeability to water [19]. Through the addition of cholesterol, the fluidity of niosomes is changed considerably [20]. Cholesterol imparts rigidity to vesicles, which is very important under severe stress conditions [21].

MATERIALS AND METHODS

Morin hydrate and cholesterol was purchased from SigmaAldrich,USA. Tween 20, Span 20 andcholesterol were received from R&M marketing; Essex, All other solvents and chemical used were of HPLC and analytical grades.

Methods of preparation [22]:

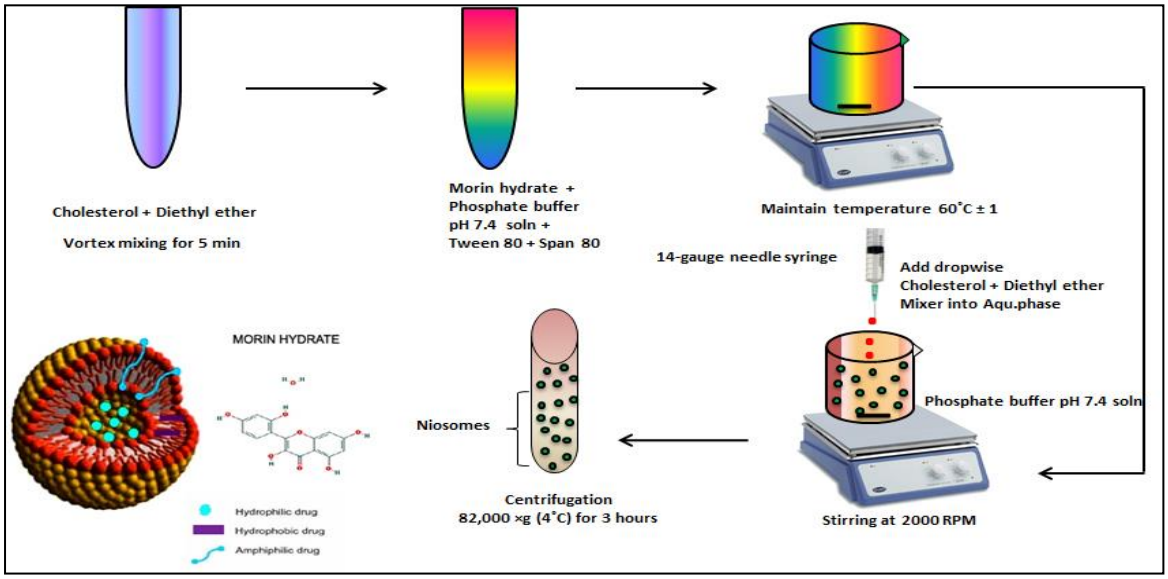

Figure-1: Preparation of morin hydrate niosomes

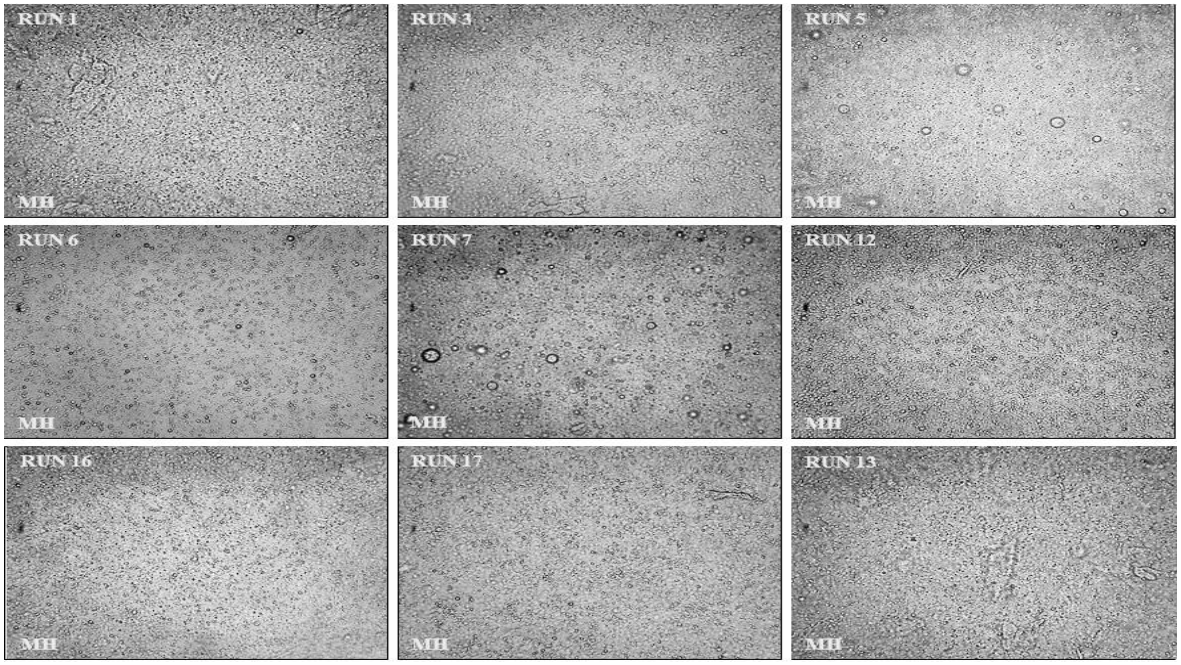

Figure-2: Optical microscopy view of various runs

Particle size analysis:

Particle size of nanoparticles was determined using malvern particle size analyzer (Zetasizer 4000S, Japan).

Viscosity Studies:

The rheological studies were performed by using brookfield viscometer (DVII+ Model pro II type-USA). The viscosity of niosomes was determined at 0.3 rpm and means of two readings were used to estimate the viscosity [23].

Drug loading efficacy:

The entrapment efficiency was determined using the ultra-centrifugation method with a slight alteration [24]. Briefly, one milliliter of niosomes was centrifuged (Avanti®J-26 XPI centrifuge) at 82,000×gfor 3 hours at 4◦C using a refrigerated ultracentrifuge so as to separate the niosomes from the non-entrapped drug. Concentration of the free drug was determined using the aforementioned HPLC method (Figure 32). RP HPLC chromatographic separation was performed on a Shimadzu liquid chromatographic system equipped with a LC-20AD solvent delivery system (pump), SPD-20A photo diode array detector, and SIL-20ACHT injector with 50µL loop volume. The LC solution version 1.25 was used for data collecting and processing (Shimadzu, Japan). The HPLC was carried out at a flow rate of 1.0 ml/min using a mobile that is phase constituted of acetonitrile, H_3PO_4 (pH 5.0) (50:50, v/v), and detection was made at 254 nm. The mobile phase was prepared daily, filtered through a 0.45µm membrane filter (Millipore) and sonicated before use. A Thermo C18 column (25cm × 4.6mm i.d., 5µ) was used for the separation. The % of drug entrapment in niosomes was calculated according to the following equation [25]:

$$\text{Drug Entrapment \%} = \left[\frac{\text{Total Drug} - \text{Drug in supernatant}}{\text{Total Drug}}\right] \times 100$$

In vitro release studies:

The release of morin hydrate from niosomes was examined under sink conditions [26]. Accurate amount of niosomes were placed in dialysis bags and suspended in 50 mL of phosphate buffer saline (PBS, pH 7.4) at 37˚C, under magnetic stirring. At pre-determined time intervals, 5 mL of solution was withdrawn and the volume of receptor compartment was maintained with an equal volume of fresh PBS. The amount of drug present in the samples was determined by HPLC method.

Experimental design:

In this work, we report the successful effect on the formulation of morin hydrate noisomes. Through preliminary experiments the Drug (A), Tween 20 (B) and Span 20 (C) were identified as the most significant variables influence the viscosity, size, % CDR, and % drug loading efficacy. Among various design approaches, the Box-Behnken (BBD) has good design properties, little collinearity, rotatable or nearly rotatable; some have orthogonal blocks, insensitive to outliers and missing data. Does not predict well at the corners of the design space. Use when region of interest and region of operability nearly the same. This Box-Behnken design is appropriate for exploring quadratic response surfaces and constructing second order polynomial models. The BBD consists of simulated center points and the set of points lying at the midpoint of each edge of the multi-dimensional cube.

Seventeen runs were essential for the response surface methodology based on the BBD. Based on the experimental design, the factor combinations produced different responses as presented in Table 2. These results clearly indicate that all the dependent variables are strongly dependent on the selected independent variables as they show a wide variation among the 17 runs. Data were analyzed using Stat-Ease Design-Expert software (DX9) to obtain analysis of variance (ANOVA), regression coefficients and regression equation. Mathematical relationship generated using multiple linear regression analysis for the studied variables are expressed as shown in Table 7.

Table-1: List of Independent variable and Dependent variables in Box-Behnken design

Independent variable	**Levels**				
Variable	Name	Units	Low	Middle	High
A	Drug	mg	5	10	15
B	Tween 20	mg	200	350	500
C	Span 20	mg	200	350	500
Dependent variable	**Goal**				
R1	Viscosity	cps		Moderate	
R2	Size	nm		Minimize	
R3	Cumulative drug release	%		Moderate	
R4	Drug loading efficacy	%		100	

Table-2: Factorial design of morin hydrate niosomes formulations

Run	Factor 1 A:Drug mg	Factor 2 B:Tween 20 mg	Factor 3 C:Span 20 mg	Response 1 Viscosity cps	Response 2 Size nm	Response 3 CDR at 12 ho.. %	Response 4 Drug loading ... %
1	10	350	350	283.1	725	63.4	68.3
2	10	200	200	280.3	720	56.7	65.9
3	10	350	350	281.8	725	63.5	68
4	10	500	200	282.9	723	59.1	65.1
5	10	350	350	282.6	724	63.4	68.1
6	5	350	500	120.1	410	50.3	55.2
7	5	200	350	119.4	408	50.4	53.9
8	10	200	500	289.4	727	64.2	69.8
9	15	500	350	397.2	575	57.6	57.1
10	5	350	200	119.3	400	45.8	50.7
11	15	200	350	385.3	573	55.2	62.3
12	15	350	200	390.4	570	53.1	56.9
13	5	500	350	103.6	405	49.6	55.1
14	15	350	500	399.1	580	57.1	59.4
15	10	500	500	289.4	730	61.2	68.4
16	10	350	350	286.3	724	62.3	67.9
17	10	350	350	285.7	724	62.9	68.4

Table-3: ANOVA results of the quadratic model for the response viscosity (R1)

Source variations	Sum of Squares	DF	Mean Square	F Value	p-value Prob> F	R^2
Model	1.582	9	17572.77	3350.16	< 0.0001	0.9998
A-Drug	1.539	1	1.539	29340.52	< 0.0001	
B-Tween 20	0.21	1	0.21	0.040	0.8467	
C-Span 20	78.75	1	78.75	15.01	0.0061	
AB	191.82	1	191.82	36.57	0.0005	
AC	15.60	1	15.60	2.97	0.1282	
BC	1.69	1	1.69	0.32	0.5880	
A^2	3891.20	1	3891.20	741.84	< 0.0001	
B^2	19.01	1	19.01	3.62	0.0986	
C^2	58.42	1	58.42	11.14	0.0125	
Residual	36.72	7	5.25			

Table-4: ANOVA results of the quadratic model for the response particle size (R2)

Source variations	Sum of Squares	DF	Mean Square	F Value	p-value Prob> F	R^2
Model	2.901	9	32232.29	15092.04	< 0.0001	0.9999
A-Drug	56953.13	1	56953.13	26667.02	< 0.0001	
B-Tween 20	3.13	1	3.13	1.46	0.2657	
C-Span 20	144.50	1	144.50	67.66	< 0.0001	
AB	6.25	1	6.25	2.93	0.1309	
AC	0.000	1	0.000	0.000	1.0000	
BC	0.000	1	0.000	0.000	1.0000	
A^2	2.317	1	2.317	1.085	< 0.0001	
B^2	0.76	1	0.76	0.36	0.5695	
C^2	0.13	1	0.13	0.060	0.8130	
Residual	14.95	7	2.14			

Table-5: ANOVA results of the quadratic model for the response % of CDR at 12 h (R3)

Source variations	Sum of Squares	DF	Mean Square	F Value	p-value Prob> F	R^2
Model	543.81	9	60.42	212.81	< 0.0001	0.9964
A-Drug	90.45	1	90.45	318.57	< 0.0001	
B-Tween 20	0.13	1	0.13	0.44	0.5282	
C-Span 20	40.95	1	40.95	144.23	< 0.0001	
AB	2.56	1	2.56	9.02	0.0199	
AC	0.063	1	0.063	0.22	0.6532	
BC	7.29	1	7.29	25.68	0.0015	
A^2	365.15	1	365.15	1286.06	< 0.0001	
B^2	1.45	1	1.45	5.12	0.0581	
C^2	20.61	1	20.61	72.59	< 0.0001	
Residual	1.99	7	0.28			

Table-6: ANOVA results of the quadratic model for the response drug loading efficacy (R4)

Source variations	Sum of Squares	DF	Mean Square	F Value	p-value Prob> F	R^2
Model	656.24	9	72.92	876.99	< 0.0001	0.9991
A-Drug	54.08	1	54.08	650.45	< 0.0001	
B-Tween 20	4.80	1	4.80	57.79	0.0001	
C-Span 20	25.21	1	25.21	303.15	< 0.0001	
AB	10.24	1	10.24	123.16	< 0.0001	
AC	1.00	1	1.00	12.03	0.0104	
BC	0.090	1	0.090	1.08	0.3327	
A^2	546.72	1	546.72	6575.67	< 0.0001	
B^2	0.53	1	0.53	6.38	0.0394	
C^2	6.01	1	6.01	72.32	< 0.0001	
Residual	0.58	7	0.083			

The normality of the data could be proved through the normal % probability plot of the externally studentized residuals. If the points on the plot lie on a straight line, the residuals are normally distributed as confirmed in Figure3.

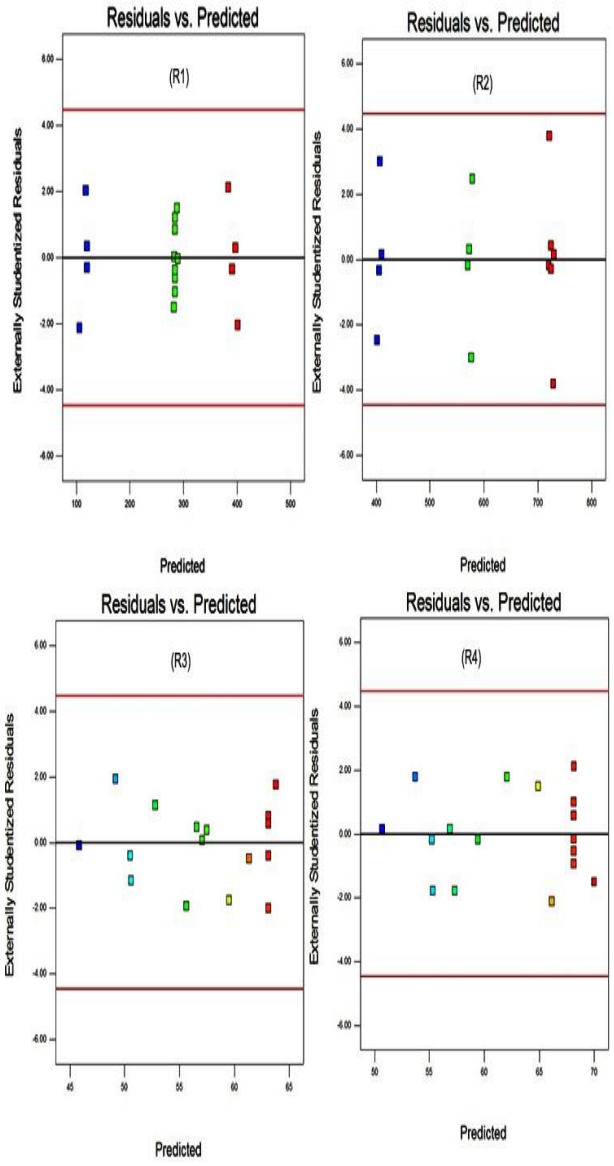

Figure-4: Residuals vs. Predicted (R1, R2, R3, R4)

The assumption of constant variance was tested by plotting externally studentized residual versus predicted values as illustrated in Figure4. The studentized residuals are located by dividing the residuals by their standard deviations. According to evident from this figure R1, R2, R3 and R4, the points are scattered randomly between the outlier detection limits - 4.5 to + 4.5.

The Residuals vs. Predicted and Residuals vs. Run were scattered randomly. From the results it can therefore be seen that the model is suitable for use and can be used to identify the optimal parameters.

R1 to R4 results show in (Figure 5) were quite satisfactory. Also, a high correlation between observed and predicted data shown indicates their low discrepancies.

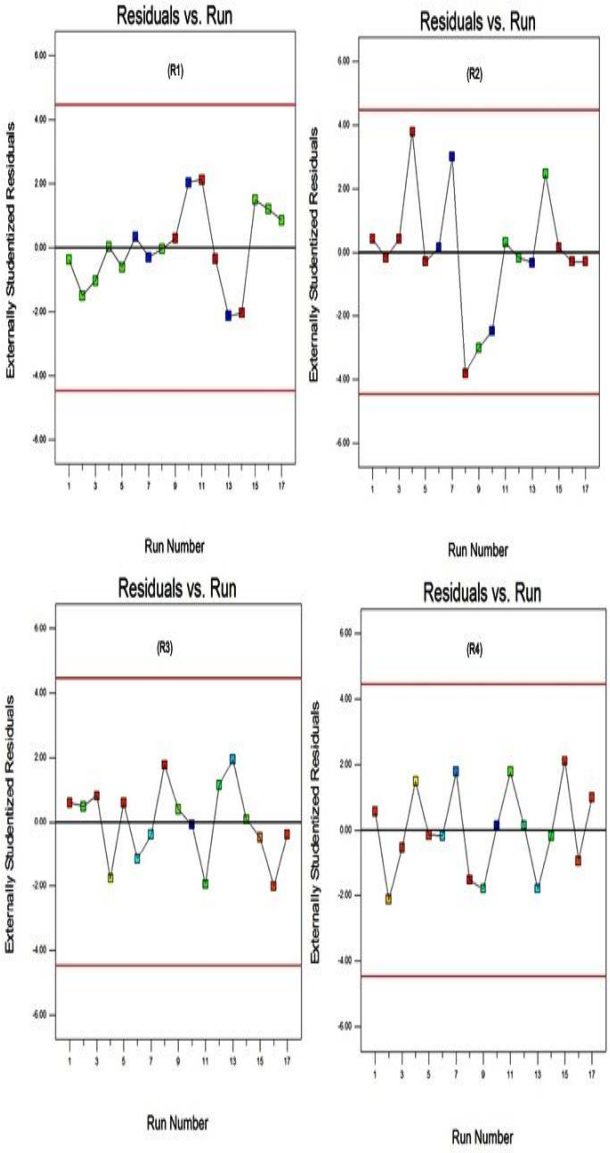

Figure -5: Residuals vs. Run (R1, R2, R3, R4)

The transformation parameter, λ, is chosen such that it maximizes the log-likelihood function. The maximum likelihood estimate of λ agrees to the value for which the squared sum of errors from the fitted model is a minimum. This value of λ is determined by fitting a numerous values of λ and choosing the value corresponding to the minimum squared sum of errors. t can also be chosen graphically from the Box-Cox normality plot. Value of λ = 1.00 indicates that no transformation needed and produces results identical

to original data shown in Figure 6.

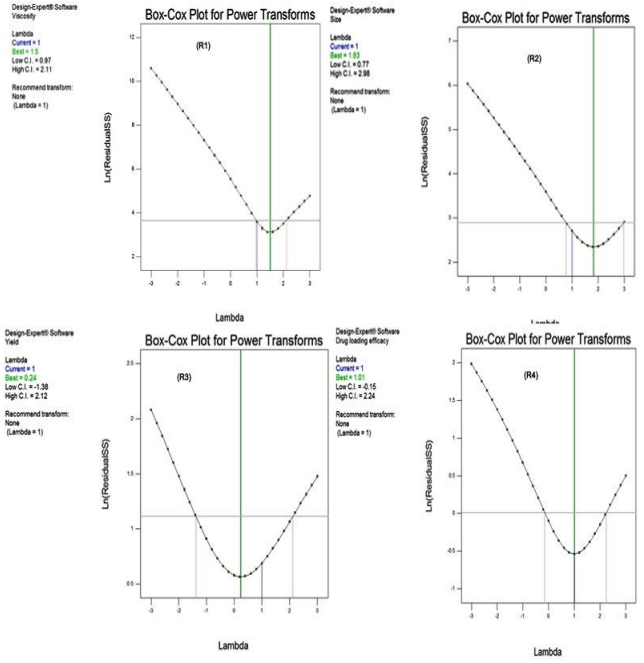

Figure -6: Box-Cox Plot (R1, R2, R3, R4)

Viscosity of morin hydrate noisomes was found to be in the range of 119.3 – 399.1 cps as shown in Table 2.The factorial equation for particle size exhibited a good correlation coefficient (1.000) and the Model F value of 3350 which implies the model is significant. Values of "Prob> F" less than 0.0500 indicate model terms are significant. In this case A, C, AB, A2 and C2 are significant model shown in Table 3. Results of the equation indicate that the effect of Drug (A) and Span 20 20 (C) are more significant than B. The influence of the main and interactive effects of independent variables on the particle size was further elucidated using the perturbation and 3D response surface plots. The individual main effects of A, B and C on viscosity are as shown in Figure 7. It is found that all the variables are having interactive effects for the response R1. The 3D response surfaces and the 2D contour plots of the response R1 are shown in Figure 8&9 to depict the interactive effects of independent variables on response R1, one variable was kept constant whereas the other two variables diverse in a certain range. The shapes of response surfaces and contour plots reveal the nature and extent of the interaction between different factors. The interaction between A and B on viscosity at a fixed level of C is shown in Figure 9. At low levels of A, R1 obtained from 120.1 to 119.3 cps. Similarly at high levels of A, R1 obtained from 390.4 to 399.1 cps. The 3-D cube plots of Box-Behnken design are as shown in Figure 10.

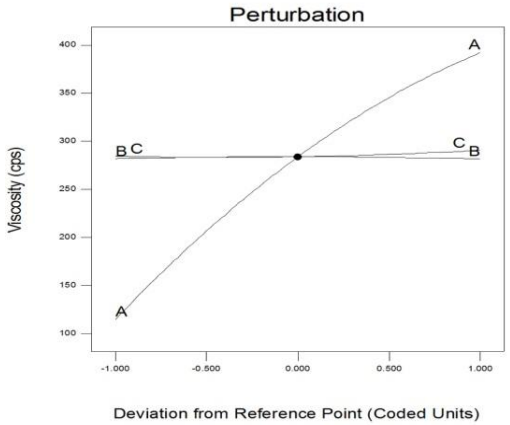

Figure-7: Perturbation plot showing the main effect of Drug (A), Tween 20 (B) and Span 20 (C) on Viscosity (R1)

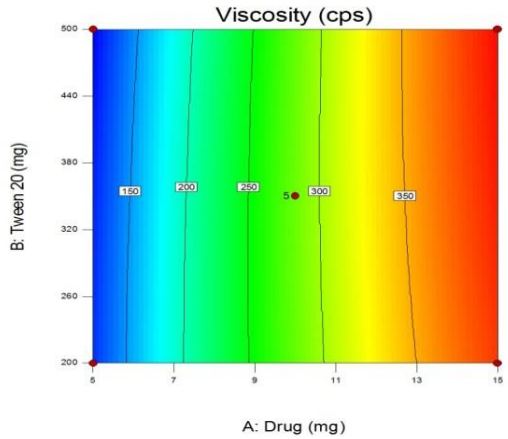

Figure-8: Response surface plot presenting the interaction between the drug and tween 20 affecting the viscosity at constant span 20 concentration(R1).

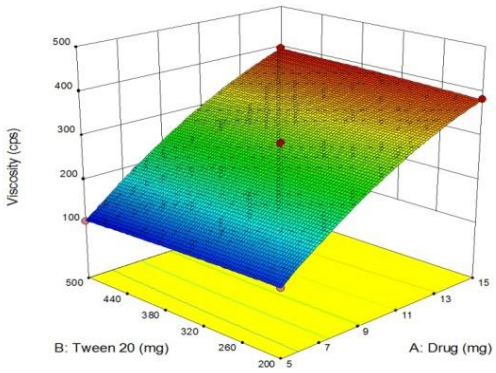

Figure-9: Response surface plot presenting the interaction between the drug and tween 20 affecting the viscosity at constant span 20 concentration(R1).

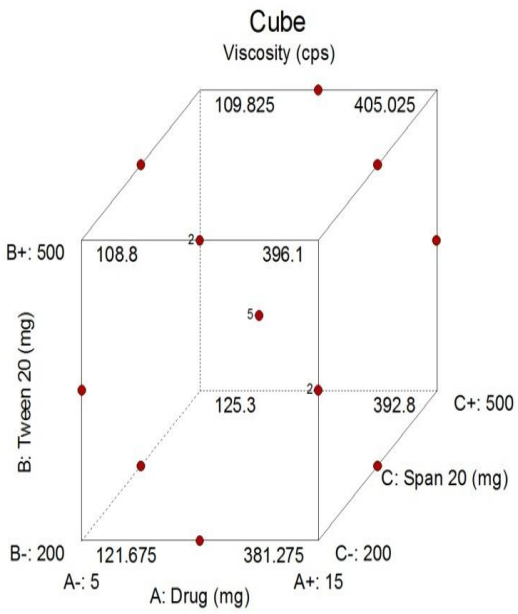

Figure -10: 3-D cube plot of Box-Behnken design (R1).

The coefficient of determination, R-squared, is a measure of the fraction of the total squared error that is explained by the model. By definition the value of R^2 varies between zero and one and the closer it is to one, the better. However, a large value of R^2 does not necessarily imply that the regression model is good one. Adding a variable to the model will always increase R^2, regardless of whether the additional variable is statistically significant or not. Thus it is possible for models that have large values of R^2 to CDR poor predictions of new observations or estimates of the mean response. To avoid this confusion, an extra statistic called the Adjusted R-squared statistic is needed; its value decreases if unnecessary terms are added. These two statistics can, when used together, imply the existence of extraneous terms in the computed model which is indicated by a large difference, usually of more than 0.20, between the values of R^2 and Adj-R^2. The amount by which the output predicted by the model differs from the actual output is called the residual. Predicted Residual Error Sum of Squares (PRESS) is a measure of how the model fits each point in the design. It is used to calculate predicted R^2. Here, the "Pred R-Squared" of 0.9998 is in reasonable agreement with the Adj R-Squared of 0.9995. Adeq Precision measures the signal to noise ratio. A ratio greater than 4 is desirable. "Adeq precision" showed (R1, R2, R3, R4) was 168.19, 293.08, 43.95 and 87.38 indicates an adequate signal respectively. This model can be used to navigate the design space. These statistics are used to prevent over fitting of model.

Subsequently producing the polynomial equations relating the dependent and independent variables, the process was optimized for the responses as shown in Table7. Mathematical optimization using the desirability approach was employed to locate the optimal settings of the process variables to obtain the desired responses. Optimized conditions were obtained by setting constraints on the dependent and independent variables. Optimization was performed to obtain the levels of A-C which moderate R1 and R3, minimize R2.

The mathematical model generated for size (R2) was found to be significant with F-value of 15092.04 ($p < 0.0001$) and R^2 value of 0.9999. The independent variables A and C the quadratic term of A^2 have significant effects on the size, since the P-values less than 0.0500 represent the significant model terms as shown in Table 5. Results of the equation indicate that the effects of A, C, A^2 are more significant. The influence of the main and interactive effects of independent variables on the size was further elucidated using the perturbation and 3D response surface plots. The perturbation plot (Figure 11) showing the main effects of A, B and C on the size (R2) of morin niosomes. This figure clearly shows that A&C has the main and the major effect on R2 followed by B which has a little effect on R2. The relationship between the dependent and independent variables was further elucidated using response surface plots; 3D response surface plot and 3-D cube plot are shown in figure 12, 13 and 14). Figure 13 shows the interactive effect of A and B on the size (R2) at fixed level of C. At low levels of A (Drug), R2 reduces from 410 to 400 nm. Similarly, at high levels of A, R2 increases from 580 to 570 nm.

Table-7: Regression equation for the response

Response	Regression equation
R1	283.90 +138.70 A – 0.16B +3.14 C +6.92 AB +1.98AC + 0.65BC -30.40 A^2 -2.12 B^2 +3.72C^2
R2	+724.40 + 84.37A +0.62B +4.25C +1.25AB -1.50AC -1.66BC -234.58A^2 +0.43B^2 –0.17C^2
R3	+63.10 + 3.36A +0.13B +2.26C +0.80AB -0.13AC -1.35BC -9.31A^2 +0.59B^2 –2.21C^2
R4	+68.14 +2.60A -0.78B +1.78C -1.60AB -0.50AC -0.15BC -11.40 A^2+0.36B^2 –1.19 C^2

Table-8: Optimized values obtained by the constraints applies on R1 to R4

Independent variables	Values	Predicted values				Code	Observed values			
		Viscosity cps (R1)	P. size (R2)	% CDR (R3)	% DLE (R4)		Viscosity cps (R1)	P. size (R2)	% CDR (R3)	% DLE (R4)
Drug	10	283.9	724.4	63.1	68.14	MH1	283.1	725	63.4	68.3
Tween 20	350					MH3	281.8	725	63.5	68.0
Span 20	350					MH17	285.7	724	62.9	68.4

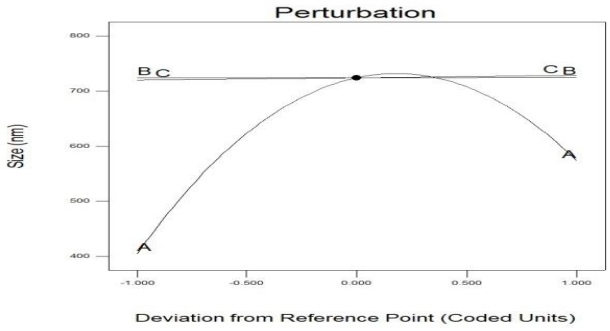

Figure-11: Perturbation plot showing the main effect of Drug (A), Tween 20 (B) and Span 20 (C) on size (R2)

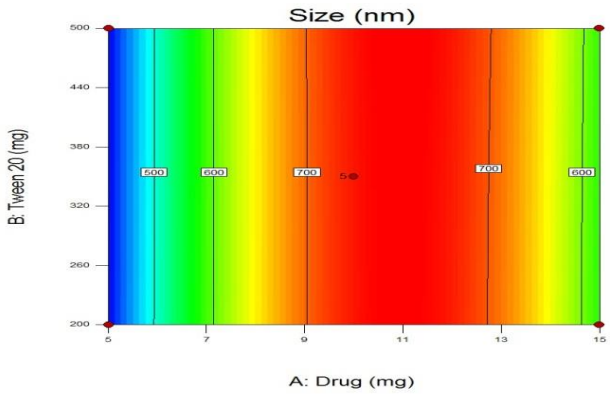

Figure-12: Response surface plot presenting the interaction between the drug and tween 20 affecting the size at constant span 20 concentration (R2).

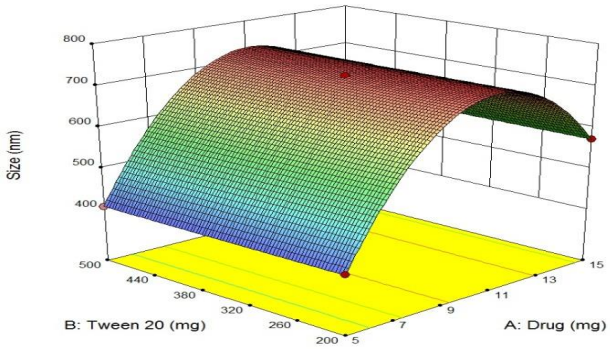

Figure-13: Response surface plot presenting the interaction between the drug and tween 20 affecting the size at constant span 20 concentration (R2).

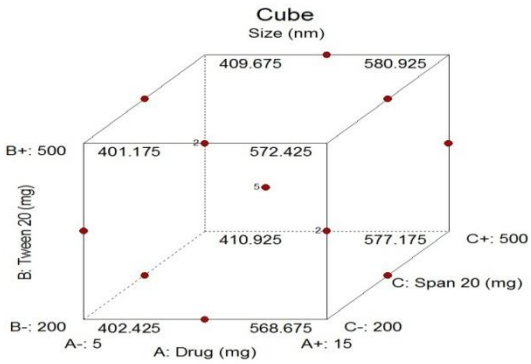

Figure -14: 3-D cube plot of Box-Behnken design (R2).

The accurate model produced for % CDR(R3) was found to be significant with F-value of 212.81 ($p < 0.0001$) and R^2 value of 0.9964. The independent variables A, B, C has significant effects on the % CDR, since the P-values less than 0.0500 represent the significant model terms as shown in Table 5. In this model A, C, AB, BC, A^2, C^2 are significant model. The perturbation plot (Figure 15) showing the main effects of A, B and C on the percentage CDR (R3) of morin niosomes. The correlation among the dependent and independent variables was further elucidated using response surface plots, response surface plot and 3-D cube plot are shown in Fig. 16, 17 and 18. Figure 17 shows the interactive effect of A and B on the % CDR(R3) at fixed level of C. At low levels of A (Drug), R3 increases from 45.8% to 50.4%. Similarly, at high levels of A, R3 increases from 53.1% to 57.6%.

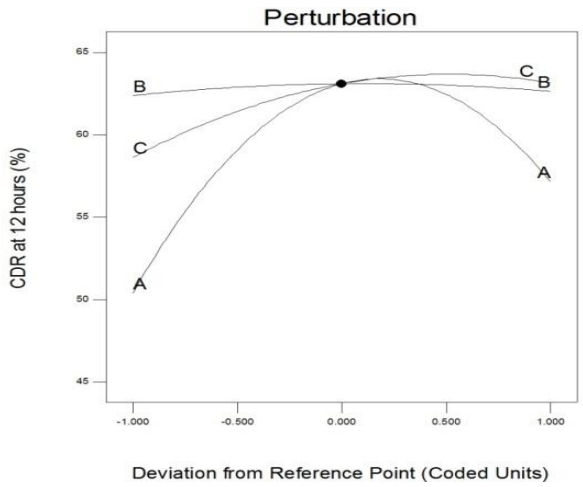

Figure-15: Perturbation plot showing the main effect of Drug (A),
Tween 20 (B) and Span 20 (C) on % CDR (R3)

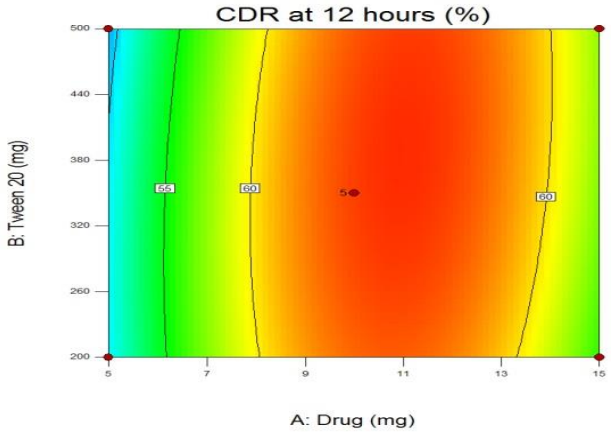

Figure-16: Response surface plot presenting the interaction between the drug and tween 20 affecting the % CDR at constant span 20 concentration (R3).

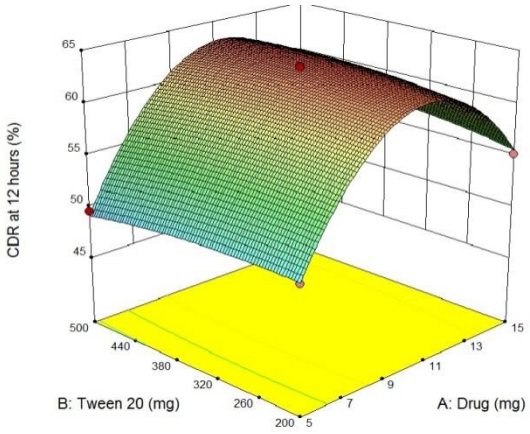

Figure-17: Response surface plot presenting the interaction between the drug and tween 20 affecting the % CDR at constant span 20 concentration (R3).

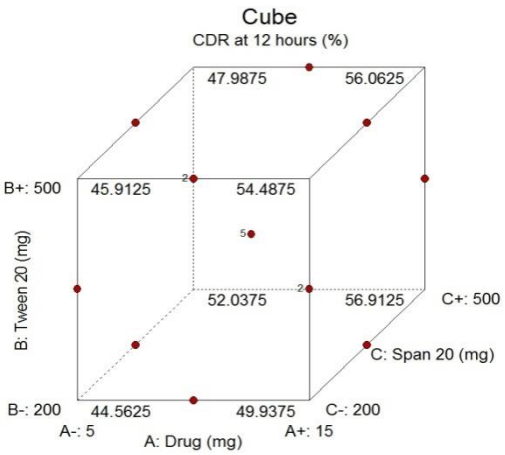

Figure -18: 3-D cube plot of Box-Behnken design (R3).

The accurate model produced for % drug loading efficacy (R4) was found to be significant with F-value of 876.99 ($p < 0.0001$) and R2 value of 0.9991. Since the P-values less than 0.0500 represent the significant model terms as shown in Table 6. In this model A, B, C, AB, AC, A^2, C^2 are significant model. The perturbation plot (Figure 15) showing the main effects of A, B and C on the viscosity (R4) of morin hydrate niosomes. The correlation among the dependent and independent variables was further elucidated using response surface plots, 3D response surface plot and 3-D cube plot are shown in Fig. 16, 17 and 18. Figure 17 shows the interactive effect of A and B on the %

drug loading efficacy (R4) at fixed level of C. At low levels of A (Drug), R3 increases from 50.7% to 55.2%. Similarly, at high levels of A, R3 increases from 56.9% to 62.3%.

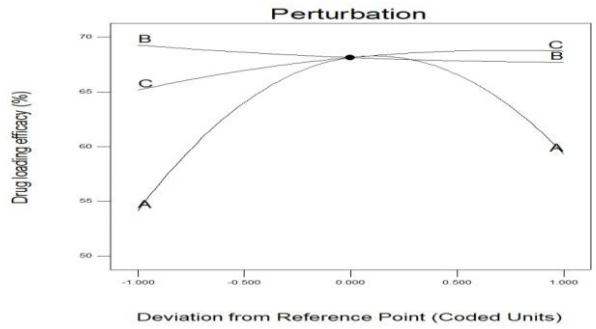

Figure-15: Perturbation plot showing the main effect of Drug (A), Tween 20 (B) and Span 20 (C) on % Drug loading efficacy (R4)

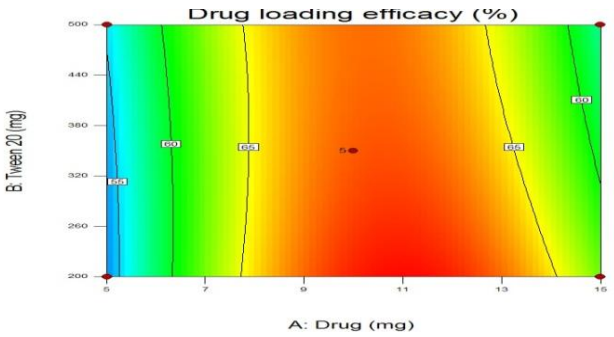

Figure-16: Response surface plot presenting the interaction between the drug and tween 20 affecting the % Drug loading efficacy at constant span 20 concentration (R4).

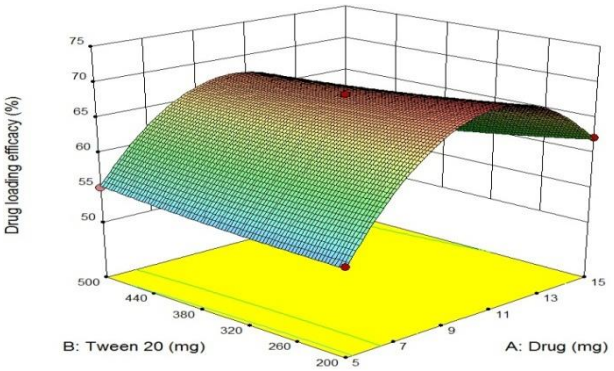

Figure-17: Response surface plot presenting the interaction between the drug and tween 20 affecting the % Drug loading efficacy at constant span 20 concentration (R4).

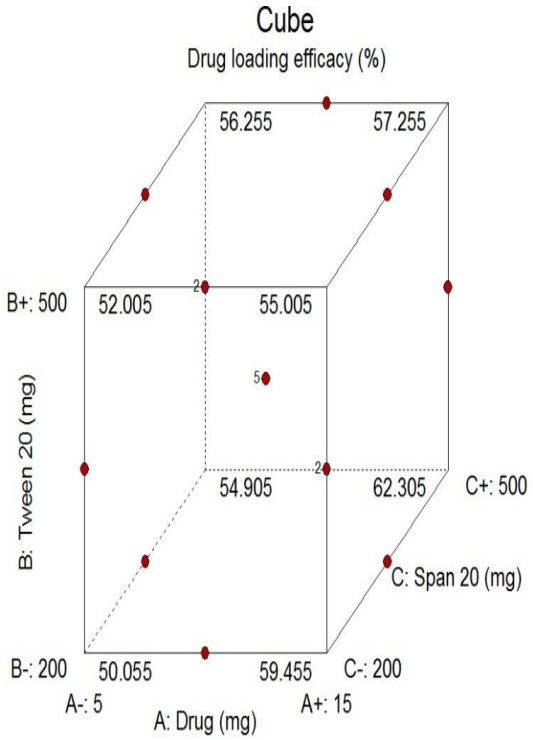

Figure -18: 3-D cube plot of Box-Behnken design (R4).

MH1, MH3 and MH17 batches code of morin hydrate niosomeswere prepared according to these optimized levels. Observed responses were in close agreement with the predicted values of the optimized process was shown in Table 8, thereby demonstrating the feasibility. The cumulative drug release from niosomes at the end of 12th hour was shown in table 2.

CONCLUSION

The tween 20 and span 20 niosomes of morin hydrate were successfully developed and optimized with the use of stat-ease design-expert software (DX9). Statistical methods based on experimental designs of tests, regression analysis and optimization techniques can be used to carry out this task moreeffectively and efficiently. To this end the implementation of a two level full factorial design and its attendant analyses are shown and explained. This work should serve as a guideline for drawing statistically valid conclusions about the optimization of noisome formulations.

REFERENCES

[1] Zhang ZT, XB Cao, N Xiong, HC Wang, JS Huang, SG Sun, T Wang.Morin exerts neuroprotective actions in Parkinson disease models in vitro and in vivo. ActaPharmacol.Sin. 31: 900–906 (2010).

[2] J Zhang, Q Peng, S Shi, Q Zhang, X Sun, T Gong, Z Zhang. Preparation,characterization, and in vivo evaluation of a self-nanoemulsifying drug deliverysystem (SNEDDS) loaded with morin–phospholipid complex. Int. J. Nanomed. 6:3405–3414 (2011).

[3] V Sivaramakrishnan,SN Devaraj. Morin fosters apoptosis in experimental hepatocellular carcinogenesis model. Chem. Biol. Interact. 183, 284–292 (2010).

[4] LSC Hsiu-MaanKuo, YL Lin, HF Lu, JS Yang, JH Lee, JG Chung.Morin inhibits the growth of human leukemia HL-60 cells via cell cycle arrest andinduction of apoptosis through mitochondria dependent pathway. Anticancer Res.395–406 (2007).

[5] XY Shuzhong Zhang,ME Morris. Flavonoids are inhibitors of breastcancer resistance protein (ABCG2)-mediated transport. Mol. Pharmacol. 65:1208–1216 (2004).

[6] Z Yu, WP Fong, CH Cheng. The dual actions of morin (3,5,7,2,4-pentahydroxy flavone) as a hypouricemic agent: uricosuric effect and xanthineoxidase inhibitory activity. J. Pharmacol. Exp. Ther. 316: 169–175 (2006).

[7] BC Choi, JS Choi, HK Han. Altered pharmacokinetics of paclitaxel by the concomitant use of morin in rats. Int. J. Pharm. 323: 81–85(2006).

[8] YJP Sang-Chul Shin, JS Choi. Effects of morin on the bioavailability of tamoxifen and its main metabolite, 4-hydroxy tamoxifen, in rats.In Vivo.391–396(2008).

[9] G Gregoriadis, AT Florence, Liposomes in drug delivery, clinical, diagnosticand ophthalmic potential, Drugs 45: 15(1993).

[10] T Yoshioka, B Sternberg, AT Florence. Int. J. Pharm. 105: 1(1994).

[11] H Schreier, J. Control. Release 30: 863(1985).

[12] H Schreier, J Bouwstra, J Control. Release 30: 1(1994).

[13] JY Fang, SY Yu, PC Wu, YB. Huang, YH. Tsai. Int. J. Pharm. 215: 91(2001).

[14] M Manconi, C Sinico, D Valenti, GLoy, AM Fadda. Int. J. Pharm. 234: 237(2002).

[15] E Touitou, HE Junginger ND Weiner, T Nagai, M Mezei, J. Pharm. Sci. 83: 1189(1994).

[16] SP Vyas, RP Singh, Int. J. Pharm. 296: 80(2005).

[17] M Manconi, C Sinico, D Valenti, F Lai, AM Fadda. Int. J. Pharm. 311: 11(2006).

[18] H Talsma, MJ Van Stenberg, JHC Brochert, D Crommelin. J Pharm Sci.83:216 (1994).

[19] Hinz HJ, Kuttenreich H, Mayer R, Renner M, Frund R. Biochemistry 1991;30:5125.

[20] Cable. Phd Thesis, University of strathelyde, Glasgow, 1989.

[21] T Liu, R Guo,WHUa, J Qui. Structure behaviors of hemoglobin in PEG6000/Tween80/Span80/H2O niosome system. Colloid Surf A PhysicochemEng Aspects.293: 255-61(2007).

[22] AG Baillie, GH Coombs, TF Dolan, J Laurie. Non-ionic surfactant vesicles, niosomes,as a delivery system for the anti leishmanial drug, sodium stibogluconate. J Pharm Pharmacol.38:502-5(1986).

[23] MVRA Maivizhi Selvi, Jaya Raja Kumar, R Kanagambikai, Lee Ali Leng, Liow Hin Teng. In-vitro and in-vivo evaluation of nanoparticles loaded temperature induced oral gel drug delivery system of acyclovir.*Rapports De Pharmacie*.1(2):81-89(2015).

[24] IF Uchegbu, Duncan R, 1997. NiosomescontainingN-(2-hydroxypropyl) methacrylamide copolymer-doxorubicin (PK1): effect ofmethod of preparation and choice of surfactant on niosome characteristics anda preliminary study of body distribution. Int. J. Pharm., 155.

[25] K Ruckmani, V Sankar. Formulation and optimization of Zidovudine nio-somes. AAPS Pharm SciTech 11: 1119–1127 (2010).

[26] L. Tavano, M. Vivacqua, V. Carito, R. Muzzalupo, M.C. Caroleo, F. Nicoletta, Col-loids Surf., B 102 (2013) 803.